AIAA JOURNAL
Vol. 34, No. 8, August 1996

Accurate Computation of Design Sensitivities for Dynamically Loaded Structures with Displacement Constraints

A. C. Paul,* A. Dutta,† and C. V. Ramakrishnan‡
Indian Institute of Technology, Delhi 110016, India

Design sensitivities for structures under transient dynamic loads with constraints on displacement can become very erroneous when proper care is not being taken in choosing the proper finite element mesh and also in selecting the appropriate number of basis modes. We approach this problem by systematically achieving an adaptive finite element mesh for a specified number of modes decided on the basis of some criteria and calculating the sensitivities thereafter. Numerous examples are solved to demonstrate how this integrated approach works and improves the results of sensitivity calculation.

Nomenclature

$\boldsymbol{B}$ = strain displacement matrix
$\boldsymbol{D}$ = constitutive matrix
$\boldsymbol{J}$ = Jacobian matrix
$\boldsymbol{K}$ = assembled stiffness matrix
$\boldsymbol{M}$ = assembled consistent mass matrix
$\boldsymbol{N}$ = shape function
$\boldsymbol{q}$ = $\boldsymbol{p}s(t)$ where $\boldsymbol{p}$ is the time-independent part of the load vector $\boldsymbol{q}$
w = Gaussian weight factor
z = nodal displacement vector
ρ = mass density
σ_g = stress vector at Gauss point

Introduction

OPTIMIZATION of structures involves the calculation of the derivatives of the objective and constraint functions with respect to design variables as one of the very important steps. The analysis and design sensitivity computations are simple in the case of static loading conditions, but for dynamic loading, the presence of inertial effects and the time-dependent load render them very complex.

Four methods of sensitivity computation have been employed traditionally for applications. The finite difference computations were employed widely in the past[1,2] on account of the simplicity in implementation. Although it is known that the method is computing intensive, it is still considered a practical algorithm on account of the ease in coding. The virtual load method, originally used by Barnett and Hermann,[3] has been extensively studied by Venkayya et al.,[4] Berke,[5] and Berke and Venkayya.[6] The state space method proposed by Haug and Arora[7] consists in first treating the displacement vector as an independent variable. An adjoint relationship is introduced to express the variation of the nodal displacement vector z in terms of the variation in design variable vector. Fox[8] and his co-workers have utilized the approach of a direct differentiation of the constraints with respect to the design variable. By using a closed form for obtaining the derivatives of the displacement vector, the design derivatives could be employed very efficiently.[9]

The details just presented refer to problems related to static analysis and mainly for skeletal structures. For problems involving frequency constraints the work of Fox and Kapoor[10] is relevant. Shape optimization problems involve several complications arising out of the discretization errors and the necessity of computing the derivatives of the stiffness matrix of the finite elements contributing to the sensitivity. Ramakrishnan and Francavilla[11] gave a systematic procedure for the computation of sensitivities in the context of an assembly of isoparametric finite elements. This approach has been followed by several researchers.[12,13] An alternate approach based on a material derivative technique has been proposed by Haug et al.[14] This method is slightly complicated on account of mathematical complexities. From the point of view of accuracy both appear to be comparable. Structural design sensitivity in the context of transient dynamic loading has been investigated by very few researchers. Feng et al.[15] proposed the solution of an adjoint system of equations based on control theoretic formulation and also advocated the use of modal superposition technique for the solution of the two systems and obtained fairly accurate design derivatives for the skeletal structural problems. Hsieh and Arora[16] proposed the adjoint variable method and used a direct integration approach for computing the design sensitivities. Simple multidegree freedom examples were discussed, although it was claimed that the method could be applied for large structural systems. Hsieh and Arora[17] present a review of the methods and also propose a worst case design formulation wherein each constraint is replaced by a set of constraints at the local maximum point. They also propose[18] a hybrid formulation in which the domain of the constraint is divided in to several subdomains, each containing one local maximum point. An equivalent functional constraint is then formulated over certain subdomains around the local maximum point. Practical applications to large structural systems indicate difficulties arising out of modal truncation in the former approach and the choice of time increment step in the later. However, it could clearly be postulated that with a proper choice of time step and inclusion of sufficient number of modes, accurate computation of sensitivities is possible for large structural systems that do not involve domain discretization errors. The problem of computing design sensitivities in a finite element context involving transient dynamic loading was addressed by Ramakrishnan et al.[19] for the purpose of solving optimum shape design problems.

Although the availability of sensitivities is a prerequisite for the use of any of the efficient gradient-based quadrically convergent algorithms, the computation of these sensitivities itself needs to be addressed carefully on account of the following reasons.

1) This computation itself is the most computing intensive step and hence the use of efficient techniques needs to be developed.

2) The errors associated with the numerical evaluation of these sensitivities have not been studied systematically, particularly for dynamic problems involving finite elements and shape variation.

In this paper, the design sensitivities are calculated following the algorithm given in Ramakrishnan et al.[19] But it is seen that the derivatives obtained are not reliable. The main objective of this paper is to analyze and quantify all of the possible numerical errors, and efforts are made to minimize these. Truss and frame problems do not possess discretization errors, and a procedure that is different

Received April 7, 1995; revision received Aug. 28, 1995; accepted for publication Sept. 5, 1995.

*Research Scholar; also Assistant Professor, Applied Mechanics Department, R.E.C. Silchar, 788010, India.

†Research Scholar; also Lecturer, Applied Mechanics Department, R.E.C. Silchar, 788010, India.

‡Professor, Department of Applied Mechanics.

from the one used by Joo et al.[20] is proposed to control modal truncation errors. For the analysis of a two-dimensional shape design derivative problem, it is seen that both modal truncation and domain discretization errors have to be kept under control for the direct and adjoint problems. Since an accurate measure for discretization errors is not well established, the measures proposed by Dutta and Ramakrishnan[21] are utilized. Using this approach the numerical errors in the direct and adjoint problems are kept under check and the design sensitivities are computed, which are found to be very accurate for problems involving displacement constraints.

Computation of Design Derivatives

In the present paper we concentrate on obtaining the design derivatives, viz., the derivatives of the objective function $J(\boldsymbol{b})$ and the various constraint ψ_i with respect to the design variables $\boldsymbol{b}$, i.e., $(\partial J/\partial \boldsymbol{b}, \partial \psi_i/\partial \boldsymbol{b})$. Although the frequency constraints are important, these are not considered here.

The constraint function for displacements can be written in vector form as

$$\boldsymbol{g}(z, \boldsymbol{b}, t) \preceq 0 \qquad \text{for all} \quad t \tag{1a}$$

In the present formulation the preceding constraint is handled by considering the integral

$$\psi_i = \int_0^T \boldsymbol{g}_i(z, \boldsymbol{b}, t)\, \mathrm{d}t \quad \text{if} \quad \boldsymbol{g}_i \prec 0 \quad \text{in} \quad t \in (0, T)$$

$$= \int_0^T \prec \boldsymbol{g}_i(z, \boldsymbol{b}, t) \succ \mathrm{d}t \quad \text{if} \quad \boldsymbol{g}_i \succ 0 \quad \text{in} \quad t \in (0, T) \tag{1b}$$

The first variation of $\psi_i(z, \boldsymbol{b})$ is

$$\delta \psi_i = \frac{\partial \psi_i}{\partial z} \delta z + \frac{\partial \psi_i}{\partial \boldsymbol{b}} \delta \boldsymbol{b} \tag{1c}$$

The second term represents the direct changes in the constraint function due to shape changes assuming the field displacements to remain unchanged, whereas the first term corresponds to the constraint function changes due to changes in field displacement. For static problems, the procedure for the computation of these sensitivities has been well researched but to date no systematic information is available for transient dynamic problems involving shape change. To express δz in terms of $\delta \boldsymbol{b}$ in Eq. (1c), we consider a small neighborhood of design space and taking a variation of equation $\boldsymbol{M}(\boldsymbol{b})\ddot{z} + \boldsymbol{K}(\boldsymbol{b})z = \boldsymbol{q}(t)$, we get

$$\boldsymbol{M}\delta\ddot{z} + \boldsymbol{K}\delta z = \left(\frac{\partial \boldsymbol{q}}{\partial \boldsymbol{b}} - \frac{\partial \boldsymbol{M}}{\partial \boldsymbol{b}}\ddot{z} - \frac{\partial \boldsymbol{K}}{\partial \boldsymbol{b}} z\right)\delta \boldsymbol{b} = \frac{\partial \boldsymbol{R}}{\partial \boldsymbol{b}} \delta \boldsymbol{b} \tag{2}$$

subject to

$$\delta \dot{z}(0) = 0 \qquad \delta z(0) = 0 \tag{3}$$

in which

$$\boldsymbol{R}(\boldsymbol{b}, t) = \boldsymbol{q}(t) - \tilde{\boldsymbol{M}}\ddot{\tilde{z}} - \tilde{\boldsymbol{K}}\tilde{z} \tag{4}$$

where the notation $\sim$ above an argument indicates that argument is held constant for the calculation. Premultiplying Eq. (2) by the transpose of an adjoint vector λ, integrating by parts over the time interval, and using Eq. (3) yield the identity

$$\lambda^T(T)\boldsymbol{M}\delta\dot{z}(T) - \dot{\lambda}^T(T)\boldsymbol{M}\delta z(T) + \int_0^1 [\ddot{\lambda}^T(t)\boldsymbol{M} + \lambda^T(t)\boldsymbol{K}]\, \delta z\, \delta t = \int_0^T \lambda^T(t) \frac{\partial \boldsymbol{R}}{\partial \boldsymbol{b}} \delta \boldsymbol{b}\, \delta t \tag{5}$$

Following the steps for formulation as an optimal control problem, we get an adjoint system

$$\boldsymbol{M}\ddot{\lambda}(t) + \boldsymbol{K}\lambda(t) = \left[\frac{\partial \boldsymbol{g}}{\partial z}\right]^T \tag{6}$$

subject to

$$\dot{\lambda}(T) = 0 \qquad \lambda(T) = 0$$

The solution of the preceding system for λ using the same eigensystem for the direct problem results in a simple procedure for the evaluation of

$$\int_0^T \frac{\partial \boldsymbol{g}}{\partial z}(z, \boldsymbol{b}, t)\, \delta z\, \mathrm{d}t \qquad \text{as} \qquad \int_0^T \left[\lambda^T \frac{\partial \boldsymbol{R}}{\partial \boldsymbol{b}}(\boldsymbol{b}, t)\, \mathrm{d}t\right]\delta \boldsymbol{b} \tag{7}$$

Thus we get

$$\delta \psi_i = \int_0^T \left\{\left[\lambda^T \frac{\partial \boldsymbol{R}(\boldsymbol{b}, t)}{\partial \boldsymbol{b}} + \frac{\partial g_i(z, \boldsymbol{b}, t)}{\partial \boldsymbol{b}}\right]\mathrm{d}t\right\}\delta \boldsymbol{b}$$

i.e.,

$$\frac{\partial \psi}{\partial \boldsymbol{b}} = \int_0^T \left[\lambda^T \frac{\partial \boldsymbol{R}(\boldsymbol{b}, t)}{\partial \boldsymbol{b}} + \frac{\partial \boldsymbol{g}(z, \boldsymbol{b}, t)}{\partial \boldsymbol{b}}\right]\mathrm{d}t \tag{8}$$

where λ represents the matrix of adjoint vector solutions for the set of constraints.

For a structural sizing problem the computation of $\partial \psi/\partial \boldsymbol{b}$ is straightforward [Eqs. (2–8)] from a mathematical viewpoint.

For shape optimization problems with displacement constraints the evaluation of $\partial \boldsymbol{R}/\partial \boldsymbol{b}$ requires further mathematical steps. To compute $\partial \boldsymbol{R}/\partial \boldsymbol{b}$ we consider Eq. (4):

$$\frac{\partial \boldsymbol{R}}{\partial b_k} = \frac{\partial \boldsymbol{q}}{\partial b_k} - \frac{\partial \boldsymbol{M}}{\partial b_k}\ddot{z} - \frac{\partial \boldsymbol{K}}{\partial b_k} z$$

Using

$$\boldsymbol{K}_e = \iint \boldsymbol{B}^T \boldsymbol{D} \boldsymbol{B}\, \mathrm{d}v = \sum_{i=1}^{ngaus} \sum_{j=1}^{ngaus} w_i w_j |\boldsymbol{J}| \boldsymbol{B}^T \boldsymbol{D} \boldsymbol{B}$$

and

$$\boldsymbol{M}_e = \int \rho \boldsymbol{N}^T \boldsymbol{N}\, \mathrm{d}v = \sum_{i=1}^{ngaus} \sum_{j=1}^{ngaus} w_i w_j \rho \boldsymbol{N}^T \boldsymbol{N} |\boldsymbol{J}|$$

and utilizing expressions for numerical quadrature

$$\boldsymbol{M}' = \Sigma_e \Sigma_i \Sigma_j \boldsymbol{N}^T \rho \boldsymbol{N} |\boldsymbol{J}|' w_i w_j$$

$$\boldsymbol{K}' = \Sigma_e \Sigma_i \Sigma_j [(\boldsymbol{B}^T \boldsymbol{D} \boldsymbol{B}' + \boldsymbol{B}'^T \boldsymbol{D} \boldsymbol{B})|J| + \boldsymbol{B}^T \boldsymbol{D} \boldsymbol{B} |J|'] w_i w_j \tag{9}$$

Thus $\boldsymbol{M}'\ddot{z}$ and $\boldsymbol{K}'z$ can be written as

$$\boldsymbol{M}'\ddot{z} = \Sigma_e \Sigma_i \Sigma_j \boldsymbol{N}^T \rho \boldsymbol{N} |\boldsymbol{J}|' \ddot{z} w_i w_j$$

$$\boldsymbol{K}'z = \Sigma_e \Sigma_i \Sigma_j \left(\boldsymbol{B}^T \boldsymbol{D} \boldsymbol{B}' z |\boldsymbol{J}| + (\boldsymbol{B}'^T |\boldsymbol{J}| + \boldsymbol{B}^T |\boldsymbol{J}|')\{\sigma_g\}\right) w_i w_j \tag{10}$$

The significance of various terms of the second part of Eq. (10) are well documented in the literature in the context of shape optimization problems. All integrations with respect to time can be performed using a suitable Newton–Cotes formula.

Computational Algorithm

It is obvious that the computational procedure has to be efficient for the computation of design derivatives. The algorithm used for the calculation of design derivatives is described as follows.

1) The control data for analysis, identification of boundary definition points, etc., should be made available.

2) In the shape optimization problem, for the given set of design variables, mesh is generated and nodal coordinate derivatives with respect to design variables $[(x_i', y_i'), i = 1, 2, \ldots,$ total number of nodal points] are also computed.

3) A finite number of eigenvectors and eigenmodes for the structural vibration problem are computed.

4) Transient dynamic response using the modal superposition technique is computed and nodal displacements at various time instants are stored.

5) It is required to carry out backward integration of the adjoint equation using the modal superposition technique since the eigenvalues and eigenvectors of the adjoint problem are the same. At each backward time step, steps 6–10 are to be performed.

6) Identify all of the elements sensitive to shape change. For each element, $\partial \boldsymbol{R}/\partial \boldsymbol{b}$ is computed using appropriate expressions.

7) For each $\{\partial \psi_i/\partial z\}$ vector the computation for incremental computation of the adjoint vector at the current backward time step is to be carried out.

8) Calculations at step 7 for each constraint derivative vector are performed and the matrix of adjoint vectors λ is obtained.

9) The inner product $\lambda^T(\partial \boldsymbol{R}/\partial \boldsymbol{b})$ is required to be computed.

10) The contribution for $\partial \psi/\partial \boldsymbol{b}$ for the time interval t to $(t+\delta t)$ is computed by numerical integration using Simpson's rule.

11) The matrix of constraint vector sensitivities $[\partial \psi_i/\partial \boldsymbol{b}_k]$ is now available.

Sources of Numerical Errors in Design Derivative Computations

It is obvious that the accuracy of design derivative computation needs very careful scrutiny. Errors can arise on account of the following: 1) discretization errors in the solution of the direct problem, 2) modal truncation errors in the solution of the direct problem, 3) numerical time integration errors, 4) errors in the computation of $\ddot{z}$, 5) errors in the computation of $\boldsymbol{K}'$ and $\boldsymbol{M}'$, 6) discretization errors in the solution of the adjoint problem, 7) modal truncation errors in the solution of the adjoint problems, and 8) errors in the numerical computation $\partial \psi/\partial \boldsymbol{b}$ using Eq. (8).

The mathematical basis of the sensitivity calculation is quite rigorous, and these errors are therefore purely numerical and computational. The eigenproblems associated with the direct and adjoint problems are identical, but the forcing functions are different. Thus the number of modes to be taken in the modal superposition analysis could be quite different for the direct and adjoint problems. At this stage, it is desirable to exclude complications arising out of discretization errors.

Considering the problem associated with skeletal structures, the stiffness and consistent mass matrices are exact. Hence discretization errors are absent, and the computation of $\boldsymbol{K}'$ and $\boldsymbol{M}'$ are also exact. Thus for the analysis of trusses and frames the errors in design sensitivity computations are 1) modal truncation errors in the solution of the direct problem, 2) errors in the computation of $\ddot{z}$, 3) modal truncation errors in the solution of adjoint problem, and 4) errors in the numerical computation of $\partial \Psi/\partial \boldsymbol{b}$ using Eq. (8).

Out of these four sources, the second one can be taken up for discussion first. Since $\ddot{z}$ involves double differentiation in time [alternatively, $\ddot{z}$ can also be obtained as $\boldsymbol{M}^{-1}(\boldsymbol{q}-\boldsymbol{K}z)$], the errors need careful study. However, the displacements z are obtained by numerical integration using Simpson's rule resulting in errors $\mathcal{O}(\Delta t^5)$; $\ddot{z}$ computation yields reliable results. This can be further confirmed by conducting a study of the variation of rms error norm as a function of Δt. Results obtained for a finite element analysis based study as reported by Dutta and Ramakrishnan[21] for a cantilever beam subjected to suddenly applied load are presented in a graphical form in Fig. 1. It is obvious that the procedure is convergent and the numerical errors due to this can be controlled by suitably controlling Δt.

Thus the principal error to be quantified and studied is the modal truncation error. In this context we liberally draw the ideas from the work referred to earlier (Dutta and Ramakrishnan[21]).

Truncation errors are introduced in the response calculation because of the introduction of a reduced system. If we take m basis modes out of the total n modes, then the load will also be represented by m modes and the error in load representation is $\boldsymbol{e}_m = \boldsymbol{p} - \boldsymbol{q}_m$ where $\boldsymbol{p}$ represents the time-independent part of applied load $\boldsymbol{q}$ and $\boldsymbol{q}_m$ is defined later. A cutoff criterion utilized in Joo et al.[20] has been compared with the results of another similar cutoff criterion. We have $\boldsymbol{q}_m = \sum_{i=1}^{m} \boldsymbol{v}_i \boldsymbol{p}^T \boldsymbol{M} \boldsymbol{v}_i$ and hence number of basis vector $\boldsymbol{v}_i$ included in the transformation is directly related to the accuracy of the solution. The cutoff criterion (Joo et al.[20]) can be written as

$$\epsilon_m = \frac{|\boldsymbol{p}^T \boldsymbol{e}_m|}{\boldsymbol{p}^T \boldsymbol{p}} \tag{11}$$

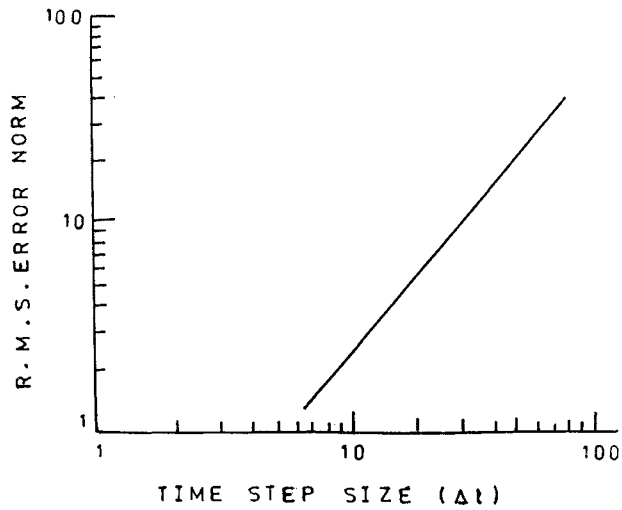

Fig. 1 Global rms error norm vs step size.

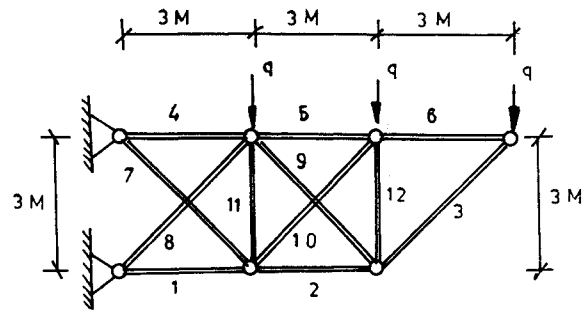

Fig. 2 Truss: $q = 1000$ N, $E = 2.0\,e\,11$ N/m^2, and $\rho = 7850$ kg/m^3.

Similarly, the cutoff criterion as proposed is given by

$$\epsilon'_m = \frac{\boldsymbol{e}_m^T \boldsymbol{e}_m}{\boldsymbol{p}^T \boldsymbol{p}} \tag{12}$$

Equation (12) as suggested here, gives a measure on magnitude of the error $\boldsymbol{e}_m$, whereas Eq. (11) as proposed by Joo et al.[20] will also involve a cosine of the angle between $\boldsymbol{q}$ and $\boldsymbol{e}_m$ vectors. This will give correct representation of the magnitude of the error when cosine term is very nearly 1. The value of $\cos\alpha$ gives a measure of error in direction.

Example 1: Truss

Consider first a 12-member truss subjected to a suddenly applied load as shown in Fig. 2. The truss has 10 degrees of freedom, and the exact solution can be obtained by including all of the modes. By storing the stresses in elements for all of the modes and carrying out the analysis with truncated modes, one can obtain the rms error for each level of truncation. It is assumed that by proper choice of Δt and effective control of tolerances, the errors due to time integration and eigenvector inaccuracies are avoided. The cutoff errors as described in Eqs. (11) and (12) can also be computed along with rms error in stresses. The modal participation factor (MPF) and the modal significance factor (MSF) (product of modal participation factor and amplification ratio) and their ratios with respect to maximum value can also be calculated. The results are shown in Table 1. It is obvious that although rms error is the correct measure, it is not realistic to compute it for practical implementation in an algorithm involving modal truncation. It is obvious that any cutoff criterion can be proposed based either on MPF or MSF or the cutoff error as per Eqs. (11) and (12).

It is obvious that by the use of a proper modal cutoff criterion based on ϵ_m or ϵ'_m or $\beta_{pm} = \text{MPF/MPF}_{\max}$ and $\beta_{sm} = \text{MSF/MSF}_{\max}$, accuracy in the computation of response can be achieved. It is now necessary that the same criterion should be applied to the adjoint problem as well for accuracy in the computation of λ. This will be discussed later. NIGEN represents number of modes, and rms error

Table 1 Modal truncation error information for truss

NIGEN	Truncation error ϵ_m	Truncation error ϵ'_m	rms error	Relative percent error	MPF	$\beta_{pm} = \text{MPF}/\text{MPF}_{\max}$
1	0.4096	0.4932	1.39e6	28.19	−5.8e−3	1.0
2	0.4193	0.4945	1.32e6	27.17	−6.1e−5	1.0e−2
3	0.4364	0.4996	1.26e6	25.79	−4.7e−5	8.1e−3
4	0.3934	0.4451	0.96e6	19.34	−5.4e−5	9.2e−3
5	0.3934	0.4446	0.96e6	19.32	−3.7e−6	6.3e−4
6	0.3946	0.4467	0.96e6	19.24	2.8e−6	4.7e−4
7	0.3225	0.3799	0.81e6	16.57	−1.8e−5	3.2e−3
8	0.3203	0.3786	0.81e6	16.51	−1.7e−6	2.9e−4
9	8.8e−5	8.5e−3	0.72e5	2.05	3.5e−5	5.9e−3
10	8.e−10	5.3e−3	0.0	0.0	−2.3e−6	3.9e−4

Table 2 Errors in design derivative calculation for the 12-bar truss with two variables (displacement constraint at node 3 and under suddenly applied load)

NIGEN	ϵ_m (direct)	ϵ_m (adjoint)	Design sensitivities by Computational analysis, $\partial\psi_i/\partial \boldsymbol{b}$	Design sensitivities by Finite difference approach, $\partial\lvert\psi_i^*/\partial \boldsymbol{b}$	Difference, %[a]
1	0.4237	0.9509	−2.70690	−2.1226	27.5
			−0.196665	−0.6511	69.79
2	0.4283	0.889	−2.58546	−2.1472	20.4
			−0.282668	−0.6238	54.69
3	0.4464	0.6965	−2.18509	−2.1457	1.84
			−0.555913	−0.587	5.29
4	0.4043	0.57562	−2.05665	−2.1266	3.29
			−0.694746	−0.6406	8.45
5	0.4039	0.4082	−2.16351	−2.1688	0.24
			−0.616809	−0.6128	0.65
6	0.3947	0.3198	−2.0283	−2.0997	3.4
			−0.718394	−0.6629	8.37
7	0.344	7.55e−2	−2.11659	−2.1536	1.72
			−0.630605	−0.602	4.75
8	0.335	6.86e−2	−2.11828	−2.1433	1.16
			−0.62821	−0.6087	3.2
9	7.1132e−5	7.932e−3	−2.13202	−2.1311	0.043
			−0.596679	−0.6052	1.41
10	6.38e−11	−5.08e−11	−2.12485	−2.123	0.0871
			−0.602872	−0.6044	0.25

[a] $(\partial\psi/\partial \boldsymbol{b} - \partial\psi^*/\partial \boldsymbol{b})/(\partial\psi^*/\partial \boldsymbol{b}) \times 100\%$.

expressed as relative percentage of exact solution is calculated in the fifth column.

Accurate Design Sensitivity Computation for Truss Problem

The 12-bar truss problem (Fig. 2) with 2 design variables (b_1 and b_2) is taken up for study. The details are as follows. It has been considered that the horizontal and vertical members (i.e., 1, 2, 4–6, 11, and 12) have the same area of cross section ($b_1 = 7.0e - 4$ m^2) and the other members (i.e., 3, 7–9, and 10) have the same area ($b_2 = 9.0e - 4$ m^2) and the time period corresponding to first frequency, $T = 0.0311155$ s. The displacement constraint function ψ_i is

$$\psi_i = \int_0^T \left(\frac{\delta}{\delta_a} - 1\right) dt \leq 0$$

where δ is displacement at the point of constraint on the structure at any time instant and δ_a is the maximum allowable displacement corresponding to the same location.

Table 2 shows the results for two design variable problems obtained by retaining a different number of modes for the analysis of the direct and adjoint problems. The truncation error measures proposed by Joo et al.[20] are also computed (for direct and adjoint loading) in columns 2 and 3. It is obvious that, with only two modes in the basis, the design derivative components contain errors on the order of 20.4 and 54.69% with respect to finite difference results. Thus even for a single constraint with 2 variables the results for the 12-bar trusses are divergent from the finite difference results. By imposing the modal cutoff criterion as stated earlier, the accuracy of design derivatives can be improved. With the progressive increase of the number of modes in the basis, the accuracy improves steadily. As indicated by the last row, when all of the modes are included in the basis, the results are exact. This is indeed the case as shown by the error values in the last column. However, inclusion of all of the modes is unrealistic, but it is obvious that at least seven fundamental modes have to be present for a reasonable level of accuracy. Further the truncation error as proposed in Eqs. (11) or (12) does not appear to be good measure for modal cutoff.

It is interesting to know that this need for the inclusion of a large number of modes for the sensitivity computations is not so obvious. Usually three or four fundamental modes are sufficient for accurate description of the response.

Let us now consider the 12-bar truss problem (Fig. 2) with three design variables (b_1, b_2, and b_3). The details are as follows. Three different areas of cross section for the members have been considered in the analysis, which are also the three design variables. Horizontal members (1, 2, 4, 5, and 6) have areas as ($b_1 = 7.0e - 4$ m^2), vertical members (11 and 12) have areas of ($b_2 = 8.0e - 4$ m^2), and the remaining members (3, 7, 8, 9, and 10) have areas equal to ($b_3 = 9.0$ m^2). Time period $T = 0.0314118$ s.

Results of a similar study are presented in Table 3. It is obvious that for this problem also accurate design derivatives (maximum error 5.18%) can be computed by retaining eight modes in the basis whereas errors of the order of 53.25% are encountered if only two

Table 3 Errors in design derivative calculation for the 12-bar truss with three variables (displacement constraint at node 3 and under suddenly applied load)

NIGEN	ϵ_m (direct)	ϵ_m (adjoint)	Design sensitivities by Computational analysis, $\partial\psi_i/\partial \boldsymbol{b}$	Design sensitivities by Finite difference approach, $\partial\psi^*/\partial \boldsymbol{b}$	Difference, %
1	0.4233	0.9506	−2.89982	−2.3776	21.96
			−0.163443	0.217	24.7
			−0.210548	−0.67	68.5
2	0.4282	0.89075	−2.79137	−2.4141	15.63
			0.169991	0.2223	23.53
			−0.298703	−0.6389	53.25
3	0.4487	0.696	−2.39065	−2.3571	1.42
			−0.176033	0.2172	18.95
			−0.571836	−0.5996	4.63
4	0.40237	0.5572	−2.2626	−2.3889	5.29
			0.17178	0.2139	19.69
			−0.71181	−0.6512	9.3
5	0.4023	0.4442	−2.39401	−2.3875	0.27
			0.192286	0.1872	2.72
			−0.628894	−0.6296	0.11
6	0.4028	0.4363	−2.356	−2.3802	1.01
			0.193581	0.1851	4.58
			−0.660132	0.6339	4.14
7	0.3638	0.111	−2.36371	−2.4536	3.66
			0.21162	0.2422	12.62
			−0.653391	−0.6107	6.99
8	0.3519	7.98e−2	−2.37346	−2.4107	1.54
			0.213906	0.2256	5.18
			−0.64554	−0.6272	8.13
9	2.44e−4	8.39e−3	−2.39553	−2.3851	0.436
			0.221812	0.2234	0.71
			−0.613825	−0.616	0.98
10	2.425e−9	2.64e−9	−2.38837	−2.388	0.015
			0.222042	0.224	0.874
			−0.620318	−0.6224	0.3351

modes are taken (Table 3). It is thus obvious that through an efficient control of the modal cutoff as proposed, accurate design derivatives can be obtained for any skeletal structure. This is a very important and interesting result.

Design Sensitivity Computations for Two-Dimensional Finite Element Dynamic Analysis Problems

With the results obtained as earlier, it is now possible to tackle the two-dimensional dynamic sensitivity analysis problems. The problem is not at all straightforward since the presence of domain discretization errors complicates the situation.

Given a finite element mesh, it is possible to control the modal truncation error in finite element analysis using the ratios of $\text{MPF}/\text{MPF}_{\max} = \beta_{pm} \preceq \delta$ and $\text{MSF}/\text{MSF}_{\max} = \beta_{sm} \prec \delta$. The terms ϵ_m and ϵ'_m give misleading results in the context of finite element discretization.[21] However, it is intuitively obvious that the errors arise due to discretization, and hence there is no guarantee that the chosen mesh is suitable for the inclusion of higher modes. At the present state of art, the only error measure and strategy available for computation of accurate dynamic response for a finite element computation are those proposed in the aforementioned reference. This is briefly discussed next.

Error Estimation

The mathematical basis and broad details of the algorithm are described in Dutta and Ramakrishnan.[21] The complete procedure of discretization error measure is given in an algorithmic form in Table 4.

Overall Strategy

Starting with a coarse mesh, the number of basis modes are first obtained, which will satisfy the cutoff criteria based on $\beta_{pm} \prec \delta$ or $\beta_{sm} \prec \delta$ adopted. Discretization errors at element level ξ'_i ($i = 1$, number of elements) are determined for these number of modes as described in the previous section. The mesh is then adaptively refined based on the ξ'_i values obtained, and the number of modes are determined, which will satisfy the cutoff criteria. Overall domain discretization error η and discretization error at element level ξ'_i are determined for a chosen number of modes. Iteration is carried out until the mesh is an optimal one satisfying the modal cutoff criteria based on β_{pm} or β_{sm} is reached.

Presently, only design derivatives of constraints on displacements of the type $\int_0^T [(\delta/\delta_a)-1]\mathrm{d}t \preceq 0$ are considered since stress constraints involve further complications of discretization errors in the adjoint problem. These will be addressed in a subsequent publication.[22]

Example 2: Cantilever Beam

A cantilever beam subjected to suddenly applied load of 6×10^5 N at the free end is chosen for design derivative calculation (Fig. 3). The depth at the fixed end of the beam is taken as variable whereas the depth at the free end is assumed to be a fixed constraint parameter. The displacement constraint is set at quarter-span. Only two basis modes are included for the analysis and the mesh assumed has only eight elements as shown in Fig. 4a. The percentage of error between $\partial\psi/\partial \boldsymbol{b}$ and $\partial\psi^*/\partial \boldsymbol{b}$ is only 0.219%. The small percentage of error does not really mean that the design derivatives calculated by both the methods are correct. If we look at η and β_{pm} for both the direct and adjoint problems, it is obvious that neither the mesh nor the number of modes are sufficient for the analysis. The same problem is again considered by taking the depth at the free end of the beam as variable while the depth at the fixed end is assumed to be a fixed parameter. The displacement constraint is set at quarter-span. The mesh is as shown in Fig. 4b. The results shown in Table 5 indicate that the percentage of error between $\partial\psi/\partial \boldsymbol{b}$ and $\partial\psi^*/\partial \boldsymbol{b}$ is as high as 85.9% when only two modes and the mesh with eight elements are taken for the analysis. The reason for such a high percentage of error can be explained next.

Table 4 Algorithm for domain discretization error

1) Solve $MV\Omega = KV$

2) Calculate dynamic response for $t = 0, T$

(2.1) For $i = 1, m$ nos. of eigenvector solve

$$y_i(t) = \frac{1}{\omega_{id}} \int_0^t f_i(\tau) e^{-\zeta_i \omega_i (t-\tau)} \sin \omega_{id}(t-\tau)\, d\tau$$

$$z_{(t)} = \sum v_i y_i(t)$$

(2.2) For $e = 1, n$ elements,

retrieve $z_{e_{(t)}}$ from $z_{(t)}$

for $j = 1$, number of Gaussian point,

calculate $\sigma^{(j)}_{e_{(t)}} = DB^{(j)} z_{e_{(t)}}$

calculate smooth stress $\sigma^{*(j)}_{e_{(t)}}$

$$e^{(j)}_{\sigma e_{(t)}} = \sigma^{*(j)}_{e_{(t)}} - \sigma^{(j)} e_{(t)}$$

$$\|e\|^{(j)}_{e_{(t)}} = \left\{ \int_\Omega \left[e^{(j)}_{\sigma e_{(t)}} \right]^T D_e^{-1} e^{(j)}_{\sigma e_{(t)}} d\Omega \right\}^{\frac{1}{2}}$$

$$\|u\|^{(j)}_{e_{(t)}} = \left\{ \int_\Omega \left[\sigma^{(j)}_{e_{(t)}} \right]^T D_e^{-1} \sigma^{(j)}_{e_{(t)}} d\Omega \right\}^{\frac{1}{2}}$$

$$\|e\|_{e_{(t)}} = \sum \|e\|^{(j)}_{e_{(t)}}$$

$$\|\bar{u}\|_{e_{(t)}} = \sum \|\bar{u}\|^{(j)}_{e_{(t)}}$$

for the whole structure

$$\|e\|_{(t)} = \left[\sum \|e\|^2_{e_{(t)}} \right]^{\frac{1}{2}}$$

$$\|\bar{u}\|_{(t)} = \left[\sum \|u\|^2_{e_{(t)}} \right]^{\frac{1}{2}}$$

3) Overall domain discretization error

$$\|e\|_{\text{av}} = \frac{\int_0^T \|e\|_{(t)} dt}{T}$$

$$\|u\|_{\text{av}} = \frac{\int_0^T \|u\|_{(t)} dt}{T}$$

$$\|u\|_{(t)} = \left[\|\bar{u}\|^2_{(t)} + \|e\|^2_{(t)} \right]^{\frac{1}{2}}$$

$$\eta = \frac{\|e\|_{\text{av}}}{\|u\|_{\text{av}}} \times 100\%$$

4) Discretization error at element level

For $i = 1, n$, elements,

$$\xi_i = \frac{\|e\|_{i_{(t)}}}{\bar{e}_m}$$

where

$$\bar{e}_m = \bar{\eta} \left[\frac{\|\bar{u}\|^2_{(t)} + \|e\|^2_{(t)}}{n} \right]^{\frac{1}{2}}$$

$$\xi_i' = \frac{\int_0^T \xi_i dt}{T}$$

If $\eta \le \bar{\eta}$ and

If $\xi_i' < 1$ for $i = 1, n$, STOP.

Else

$$h_{i_{\text{new}}} = \frac{h_{i_{\text{old}}}}{(\xi_i')_1^{1/p}}$$

Endif

Go to step 1.

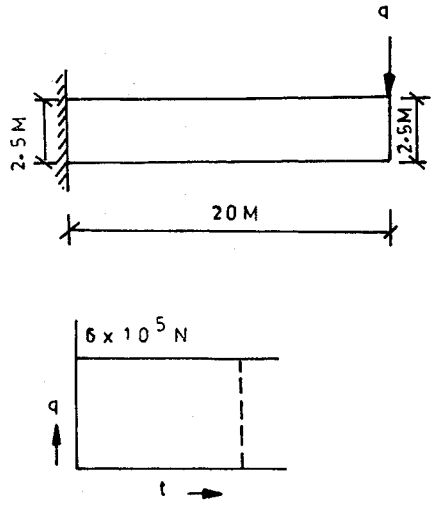

Fig. 3 Cantilever beam: E = 2.1 e 11 N/m^2, ρ = 7850 kg/m^2, and ν = 0.3.

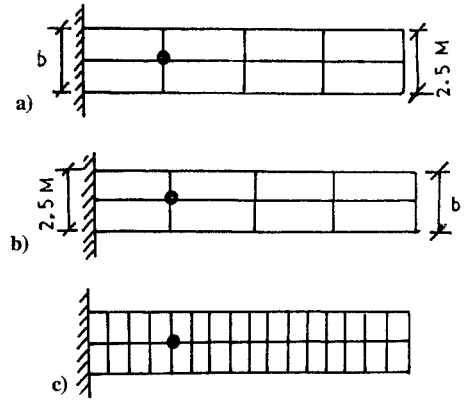

Fig. 4 Cantilever with single constraint single variable: a) variable at fixed end, b) variable at free end, and c) optimal mesh; •, constraint location.

We have

$$\frac{\partial \psi}{\partial b} = \int_0^T \lambda^T \frac{\partial R^*(b,t)}{\partial b}\, dt$$

If the error in $\partial\psi/\partial b$ is de, then

$$de = \int_0^T \left[d\lambda^T \frac{\partial R(b,t)}{\partial b} + \lambda^T d \frac{\partial R(b,t)}{\partial b} \right] dt$$

where $d\lambda$ and $d[\partial R(b,t)/\partial b]$ indicate errors in adjoint and direct solutions, respectively. If the magnitude of $[\partial R(b,t)/\partial b]$ is very large for a problem, then this will act as an amplification factor for the error in the adjoint problem, and unless the errors in adjoint problem are brought down to a very low value, the percentage of error between $\partial\psi/\partial b$ and $\partial\psi^*/\partial b$ will be projected as very high. This was the reason why we obtained only 0.219% of error in the first case whereas the error was 85.9% in the next case. By keeping $\beta_{pm} \prec 5e-3$, we need to include 7 basis modes for improved solution and the optimal mesh with 32 elements obtained by uniform refinement for $\bar{\eta} = 5\%$. The result shown in the last column of the last row of Table 5 indicates a dramatic improvement in the result as the percentage difference has come down to 3.74% only. The optimal mesh is shown in Fig. 4c. A similar study has been carried out for a tapered cantilever beam subjected to a harmonic loading of exciting frequency $\bar{\omega} = 150$ rad/s. Initial mesh has only eight elements and the mesh is shown in Fig. 5a. The depth at the midspan has been taken as variable and the constraint is set at quarter-span. The percentage of error between and $\partial\psi/\partial b$ and $\partial\psi^*/\partial b$ is 34.17% when only two basis modes are included (Table 6). A refined mesh as shown in Fig. 5b with 16 elements is obtained adaptively for $\bar{\eta} = 5\%$ and 7 basis modes satisfying the modal cutoff criterion are

Table 5 Errors in design derivative calculation for cantilever beam [displacement constraint at quarter span and under suddenly applied load (lateral)]

Mesh	NIGEN	No. of elements	Design derivatives by: Computational analysis, $\partial\psi/\partial b$	Design derivatives by: Finite difference approach, $\partial\psi^*/\partial b$	Difference, %
Fig. 4a	2	8	$-0.125889e-1$	$-0.125614e-1$	0.22
Fig. 4b	2	8	$-0.242530e-3$	$-0.130449e-3$	85.92
Fig. 4c	7	32	$-0.249537e-3$	$-0.240549e-3$	3.74

Table 6 Errors in design derivative calculation for cantilever beam [displacement constraint at quarter span and under harmonic load (lateral)]

Mesh	NIGEN	No. of elements	Design derivatives by: Computational analysis, $\partial\psi/\partial b$	Design derivatives by: Finite difference approach, $\partial\psi^*/\partial b$	Difference, %
Fig. 5a	2	8	$-0.263618e-4$	$-0.196481e-4$	34.17
Fig. 5b	11	18	$-0.103060e-4$	$-0.107515e-4$	4.14

Table 7 Errors in design derivative calculation for cantilever beam (multiple variable and single constraint)

Mesh	NIGEN	No. of elements	Design derivatives by: Computational analysis, $\partial\psi/\partial b_i$	Design derivatives by: Finite difference approach, $\partial\psi^*/\partial b_i$	Difference, %
Fig. 5a	2	8	$-0.377271e-2$	$-0.416367e-2$	9.39
			$-0.367006e-2$	$-0.276593e-2$	32.69
			$-0.149073e-3$	$-0.343105e-3$	56.55
			$0.571782e-3$	$0.383799e-3$	48.98
			$0.399050e-3$	$0.456809e-3$	12.64
Fig. 6b	7	24	$-0.435512e-2$	$-0.439999e-2$	1.02
			$-0.280669e-2$	$-0.274023e-2$	2.42
			$-0.403122e-3$	$-0.364775e-3$	10.50
			$0.393370e-3$	$0.368539e-3$	6.74
			$0.444108e-3$	$0.434878e-3$	2.12

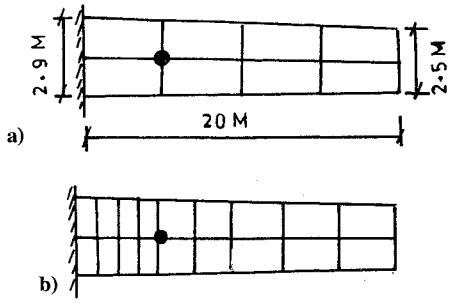

Fig. 5 Tapered cantilever with single variable and single constraint: a) starting mesh and b) optimal mesh.

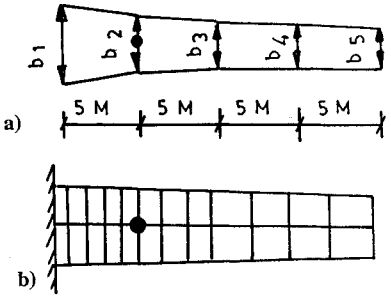

Fig. 6 Tapered cantilever with five variables and single constraint: a) problem description and b) optimal mesh: b_1 = 2.9 M, b_2 = 2.8 M, b_3 = 2.7 M, b_4 = 2.6 M, b_5 = 2.5 M.

adopted. Here also, the percentage difference of error comes down to 4.14% (Table 6).

The same tapered cantilever beam (Fig. 5a) is again considered, which is subjected to suddenly applied load. The depths at the free end, three-quarters span, midspan, quarter span, and fixed end have been taken as variables giving rise to a five variables design sensitivity problem and the constraint has been set at quarter span (Fig. 6a).

The results shown in Table 7 indicate that errors between $\partial\psi/\partial b$ and $\partial\psi^*/\partial b$ are quite high when only two basis modes and the mesh with eight elements are used. The errors can be controlled by considering appropriate mesh and adequate number basis modes following the strategy mentioned earlier. Figure 6b is obtained adaptively for $\bar{\eta} = 5\%$ and 7 basis modes for $\beta_{pm} < 5.0e-3$. Table 7 shows the percentage of errors has come down to considerably low values. It is to be mentioned here that only a systematic approach consisting of retaining a higher number of modes along with adaptive mesh refinement for discretization error control could lead to the correct results.

We next consider a 16-elements tapered cantilever beam (Fig. 7b) for multiple variables and multiple constraints. Depths at free end, three-quarters span, quarter span, and fixed end have been

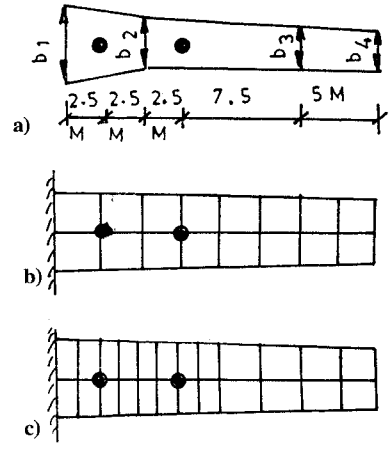

Fig. 7 Tapered cantilever with four variables and two constraints: a) problem description, b) starting mesh, and c) optimal mesh: b_1 = 2.9 M, b_2 = 2.8 M, b_3 = 2.6 M, b_4 = 2.5 M.

Table 8 Errors in design derivative calculation for cantilever beam (multiple variable and two constraints)

Mesh	NIGEN	No. of elements	Design derivatives by: Computational analysis, $\partial\psi/\partial b_i$ — First constraint	Computational analysis, $\partial\psi/\partial b_i$ — Second constraint	Finite difference approach, $\partial\psi^*/\partial b_i$ — First constraint	Finite difference approach, $\partial\psi^*/\partial b_i$ — Second constraint	Difference, % — First	Difference, % — Second
Fig. 7b	2	16	$-0.746293e-2$	$-0.112478e-2$	$-0.786710e-2$	$-0.134123e-2$	5.14	16.1
			$-0.778147e-2$	$-0.978024e-3$	$-0.732802e-2$	$-0.493012e-3$	6.19	98.4
			$0.102174e-2$	$0.187307e-3$	$0.824953e-3$	$0.104557e-3$	23.85	79.1
			$0.840469e-3$	$0.108576e-3$	$0.918806e-3$	$0.130697e-3$	8.53	16.9
Fig. 7c	12	24	$-0.793919e-2$	$-0.134558e-2$	$-0.793631e-2$	$-0.136261e-2$	0.04	1.3
			$-0.728961e-2$	$-0.526210e-3$	$-0.735254e-2$	$-0.486331e-3$	0.86	8.2
			$0.790406e-3$	$0.964459e-4$	$0.779992e-3$	$0.101955e-3$	1.33	5.4
			$0.943593e-3$	$0.113978e-3$	$0.903273e-3$	$0.118549e-3$	4.46	3.8

considered as variables. Constraints are set at one-eighth span and three-eighths span (Fig. 7a). Results shown in Table 8 indicate again large errors when only two modes are considered. The optimal mesh obtained adaptively (Fig. 7c) with 12 modes in the basis is considered for improved solution. Table 8 shows that the error percentages have reduced considerably when the mesh satisfies discretization error control requirement and the number of modes satisfying modal cutoff requirements are incorporated.

Conclusion

Design derivative calculations are very highly sensitive to the number of basis modes being used and the mesh adopted for the analysis. A systematic study is required for the determination of domain discretization error η and number of basis modes required, for both direct and adjoint problems. It is clear from the results of the truss problem that the number of basis modes plays a very important role for the improvement of design derivative results. The study of the cantilever beam problem also clearly indicates that an optimal mesh and the proper number of basis modes are absolutely essential to arrive at an accurate value of design derivatives.

References

[1]Moe, J., "Penalty Function Methods in Optimum Structural Design—Theory and Application," *Optimum Structural Design*, edited by R. H. Gallaghar and O. C. Zienkiewicz, Wiley, New York, 1973, pp. 143–177.

[2]Kavlie, D., "Optimum Design of Statically Indeterminate Structures," Ph.D. Thesis, Univ. of California, Berkeley, Berkeley, CA, 1971.

[3]Barnett, R. L., and Hermann, P. C., "High Performance Structures," NASA CR-1038, May 1968.

[4]Venkayya, V. B., Knot, N. S., and Berke, L., "Application of Optimality Criteria Approaches to Automated Design of Large Practical Structures," *2nd Symposium on Structural Optimization*, AGARD-CP-123, April 1973.

[5]Berke, L., "An Efficient Approach to the Minimum Weight Design of Deflection Limited Structures," U.S. Air Force Flight Dynamics Lab., AFFDL TM-70-4-FDTR, Wright–Patterson Air Force Base, OH, May 1970.

[6]Berke, L., and Venkayya, V. B., "Review of Optimality Criteria Approaches to Structural Optimization," *ASME Structural Optimization Symposium*, AMD Vol. 7, 1974, pp. 23, 24.

[7]Haug, E. J., and Arora, J. S., *Applied Optimal Design: Mechanical and Structural Systems*, Wiley-Interscience, New York, 1979.

[8]Fox, R. L., *Optimization Methods for Engineering Design*, Addison–Wesley, Reading, MA, 1971.

[9]Schmit, L. A., and Miura, H., "A New Structural Analysis/Synthesis Capability—ACCESS I," *AIAA Journal*, Vol. 14, No. 5, 1976, pp. 661–671.

[10]Fox, R. L., and Kapoor, M. P., "Structural Optimization in the Dynamic Response Regime: A Computational Approach," *AIAA Journal*, Vol. 8, No. 10, 1970, pp. 1798–1804.

[11]Ramakrishnan, C. V., and Francavilla, A., "Structural Optimization Using Penalty Function," *Journal of Structural Mechanics*, Vol. 3, No. 4, 1974, pp. 403–422.

[12]Kristensen, E. S., and Madsen, N. F., "On the Optimum Shape of Fillets in Plates Subjected to Multiple Inplane Loading Cases," *International Journal for Numerical Methods in Engineering*, Vol. 10, No. 5, 1976, pp. 1006–1019.

[13]Bhavikatti, S. S., and Ramakrishnan, C. V., "Optimum Shape Design of Rotating Discs," *International Journal of Computers and Structures*, Vol. 11, No. 5, 1980, pp. 397–401.

[14]Haug, E. J., Choi, K. K., and Komkov, V., *Design Sensitivity Analysis of Structural Systems*, Academic, New York, 1986.

[15]Feng, T. T., Arora, J. S., and Haug, E. J., Jr., "Optimal Structural Design Under Dynamic Loads," *International Journal for Numerical Methods in Engineering*, Vol. 11, No. 1, 1977, pp. 35–53.

[16]Hsieh, C. C., and Arora, J. S., "Structural Design Sensitivity Analysis with General Boundary Conditions: Dynamic Problems," *International Journal for Numerical Methods in Engineering*, Vol. 21, No. 2, 1985, pp. 267–283.

[17]Hsieh, C. C., and Arora, J. S., "Design Sensitivity Analysis and Optimization of Dynamic Response," *Computer Methods in Applied Mechanics and Engineering*, Vol. 43, No. 2, 1984, pp. 195–219.

[18]Hsieh, C. C., and Arora, J. S., "An Efficient Method for Dynamic Response Optimization," *AIAA Journal*, Vol. 23, No. 9, 1985, pp. 1454–1456.

[19]Ramakrishnan, C. V., Paul, A. C., and Sehegal, D. K., "Optimum Design Under Transient Dynamic Loading," *The Finite Element Methods in 1990's*, edited by E. Onate, J. Periaux, and A. Samuelsson, Springer–Verlag, Barcelona, Spain, 1991, pp. 202–211.

[20]Joo, K. J., Wilson, E. L., and Leger, P., "Ritz Vectors and Generation Criteria for Mode Superposition Analysis," *Earthquake Engineering and Structural Dynamics*, Vol. 18, No. 2, 1989, pp. 149–167.

[21]Dutta, A., and Ramakrishnan, C. V., "Error Estimation in Finite Element Transient Dynamic Analysis Using Modal Superposition Method," *Engineering Computation* (to be published).

[22]Dutta, A., and Ramakrishnan, C. V., "Accurate Computation of Design Sensitivities for Structures Under Transient Dynamic Loads with Constraints on Stresses," *International Journal of Computers and Structures* (to be submitted).